Journal of Engineering Research and Technological Innovations.
[JERTI] Vol. 1, No 2, 1 - 7 (2026)
https://journals.kwasu.edu.ng/index.php/jerti ISSN: 3093-0863

Particulate Matter Deposition Inducing Heavy Metal Enrichment and Hydrochemical Degradation near a Cement Facility in North-Central Nigeria

T. Abadunmi[1]*, A. O. Ogunlela[2], K. O. Yusuf[2]

[1]Department of Agricultural Engineering, Division of Agricultural Colleges, Ahmadu Bello University, Zaria, Nigeria
[2]Department of Agricultural and Biosystems Engineering, University of Ilorin Ilorin Nigeria

[1]tabadunmi@abu.edu.ng, [2]aogunlela@unilorin.edu.ng, [2]yusuf.ok@unilorin.edu.ng
*Corresponding Author: tabadunmi@abu.edu.ng | +234-703-737-6991

ABSTRACT

Cement production is a major source of airborne particulate matter (PM) and trace metals that can compromise the hydrogeochemical quality of surrounding ecosystems. This study evaluates PM deposition, heavy metal accumulation, soil and water quality deterioration within a 10 km radius of a cement facility in North-Central Nigeria. Results reveal evidently elevated PM deposition along production corridors (up to 9,336 µg/cm^2/day) and widespread exceedances of USEPA/NIS limits for Pb, Cd, As, and Hg across environmental media. Electrical conductivity (EC) shows a strong positive correlation with total dissolved solids (TDS, r = 0.85), while PM deposition is significantly associated with lead (Pb, r = 0.62), indicating linked pathways of particulate and ionic contamination. Collectively, cement-derived emissions drive soil alkalinization, aqueous ionic enrichment, and sustained atmospheric deposition, jointly accelerating hydrochemical degradation in the surrounding environment.

Keywords: Cement dust, cross-media contamination, hydrogeochemistry, Soil alkalinity; Water quality.

1. INTRODUCTION

Cement production is fundamental to infrastructure development but remains a major source of airborne particulate matter (PM) and trace-metal emissions that degrade environmental quality (Etim *et al.*, 2021; Ogunbiyi *et al.,* 2022). Fine particulates ($PM_{2.5}$ and PM_{10}) generated during clinker production and material handling are dispersed and deposited on surrounding soils and water bodies, introducing alkaline constituents and potentially toxic elements (PTEs) such as Pb, Cd, Cr, As, and Hg (Ismail, 2023; Yang *et al.,* 2024). These inputs modify soil and water systems by increasing alkalinity and ionic strength, thereby enhancing metal mobility and posing risks to groundwater quality and agricultural productivity.

Evidence from cement-producing regions in Nigeria consistently shows elevated PM concentrations and significant heavy metal enrichment in environmental media, with contamination levels decreasing with distance from emission sources (Adeniyi *et al.,* 2022; Ogunkunle et al., 2021; Okoro *et al.,* 2022). Although these studies establish atmospheric deposition as a primary pathway of contamination, they are largely constrained to single-media assessments and do not adequately resolve the coupled interactions between particulate deposition and hydrochemical processes across soil and water systems.

A critical research gap therefore lies in quantitatively linking PM deposition with cross-media heavy metal enrichment and hydrochemical degradation, particularly under tropical environmental conditions.

This study addresses this limitation by investigating particulate matter deposition and associated hydrogeochemical responses within a 10 km radius of a cement facility in North-Central Nigeria. Specifically, it quantifies the spatial variability of PM deposition,

Publisher
Faculty of Engineering and Technology,
Kwara State University, Malete. P.M.B. 1530 Ilorin,
Kwara State, Nigeria.

https://doi.org/10.5281/zenodo.21704216

evaluates heavy metal distribution across soil, surface water, and groundwater systems, and characterizes key physicochemical and hydrochemical parameters. It further examines the relationships between PM deposition, ionic enrichment, and metal mobility to establish cross-media contamination pathways. The study is guided by the hypotheses that PM deposition from cement production significantly elevates heavy metal concentrations across environmental media, induces measurable hydrochemical alteration reflected in increased electrical conductivity, total dissolved solids, and alkalinity, and exhibits significant positive relationships with trace metal enrichment, indicating coupled particulate–hydrochemical contamination dynamics.

2. MATERIALS AND METHODS

2.1 Study Area

The study was conducted around a cement production facility in North-Central Nigeria, located between latitudes 7°54′N–7°56′N and longitudes 6°24′E–6°27′E (Figure 1). The region is characterized by a tropical wet-and-dry climate (Aw, Köppen classification), with distinct dry (November–March) and wet (April–October) seasons. Mean annual rainfall ranges from 1,100 to 1,300 mm, while average temperatures vary between 26 and 32 °C. Prevailing wind patterns are predominantly north-easterly during the dry season (mean wind speed: 2.8 – 3.6 m/s) and south-westerly during the wet season (mean wind speed: 1.5 – 2.4 m/s), influencing particulate dispersion and deposition gradients (NiMet, 2023).

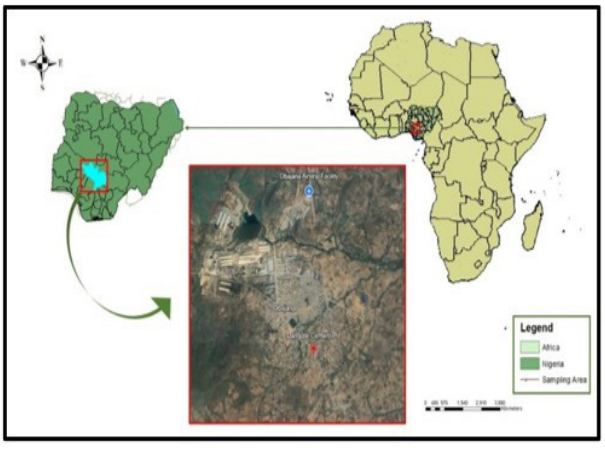

Figure 1: The Study Area

Geologically, the area lies within the Nigerian Precambrian Basement Complex, comprising migmatite–gneiss, schists, granitic intrusions, and dolerite dykes, which control soil formation and groundwater flow dynamics (Obaje, 2009). The study area includes mixed land uses (industrial, agricultural, and residential), with documented concerns regarding cement dust-induced soil degradation and groundwater contamination (Ibrahim et al., 2021; Ogunbiyi *et al.,* 2022).

2.2 Sampling Design and Data Collection

2.2.1 Particulate Matter Sampling and Characterization

Atmospheric PM deposition was assessed using passive dustfall collectors (petri-dish method) deployed at nine monitoring stations arranged radially around the cement plant. The sampling network encompassed both dominant downwind (n = 5) and upwind (n = 4) directions along a distance gradient of 0.1–5 km to capture spatial variability in particulate dispersion and deposition.

At each station, three collectors (n = 3) were installed at a standardized height of 3 m above ground level and composited to obtain representative samples, yielding 27 PM sampling units per season and 9 composite samples per season. Sampling was conducted during both dry and wet seasons in accordance with standard environmental monitoring protocols (WHO, 2013; USEPA, 2016).

The dry season enhances particulate accumulation due to atmospheric stability, whereas wet-season precipitation promotes washout and redistribution processes (Etim *et al.,* 2021). Deposition flux was determined gravimetrically and expressed as μg/cm²/day.

2.2.2 Soil Sampling and Geochemical Analysis

Soil samples were collected from 19 farmland locations along the PM deposition gradient. At each site, composite topsoil samples (0–30 cm) were obtained from three random points (n = 3 per location) using stainless-steel corers following ASTM D6044 guidelines (ASTM, 2002). Sampling was conducted in both dry and wet seasons, yielding 114 subsamples, which were composited into 19 representative samples per season.

Samples were air-dried, sieved (<2 mm), homogenized, and stored prior to analysis. Physicochemical parameters including pH, electrical conductivity (EC), organic matter (OM), and cation exchange capacity (CEC) were determined using standard laboratory procedures (Minkina *et al.,* 2018). Trace metals were analyzed following acid digestion (HNO_3–$HClO_4$) using Atomic Absorption Spectrophotometry (AAS).

2.2.3 Water Sampling and Hydrogeochemical Analysis

A total of 52 water samples were collected, comprising 49 groundwater samples (17 boreholes and 32 wells) and 3 surface water samples. Sampling was conducted during both dry and wet seasons, resulting in 104 total samples. Sampling followed established protocols (APHA, 2017; ASTM, 2001; USEPA, 2016). Samples were filtered (0.45 µm), acidified (pH < 2), refrigerated at 4 °C, and analyzed within 48 hours. A total of 26 hydrochemical parameters were determined, including major ions, trace metals, EC, total dissolved solids (TDS), alkalinity, and hardness. Analytical techniques included ion chromatography and AAS.

2.3 Quality Assurance and Quality Control (QA/QC)

Comprehensive QA/QC protocols were implemented to ensure analytical accuracy, precision, and reproducibility in accordance with established standard methods (APHA, 2017). Field and reagent blanks were employed to detect potential contamination during sampling and laboratory procedures. Instrument calibration was conducted using certified reference standards, with calibration curves achieving correlation coefficients ($R^2 \geq 0.995$).

Recovery efficiency was assessed through spike-recovery tests, yielding acceptable recoveries within 85–115%, while analytical precision was evaluated using duplicate samples (≥10% of total samples), maintaining relative percent differences below 10%. Accuracy was further verified using standard reference materials.

For hydrochemical analyses, ionic balance error (IBE) was computed and maintained within ±5%, confirming the reliability of major ion determinations (APHA, 2017). Method detection limits for trace metals were established prior to analysis, and all reported concentrations exceeded these thresholds.

2.4 Data Analysis

All datasets were processed using R (version 4.3) and SPSS (version 26). Descriptive statistics, including mean, standard deviation, and variance, were used to summarize particulate deposition, soil properties, and hydrochemical characteristics. Spatial variability was evaluated along established transects to capture gradients in particulate dispersion and contaminant distribution.

Pearson correlation analysis was applied to assess relationships between physicochemical parameters and trace metal concentrations, enabling identification of co-mobilization patterns across environmental media. Statistically significant relationships, particularly between EC and TDS ($p < 0.01$) and between PM deposition and Pb concentrations, were used to infer linkages between particulate inputs, ionic enrichment, and metal mobility processes (Etim *et al.,* 2021; Ogunbiyi *et al.,* 2022)

3.0 RESULTS AND DISCUSSION

3.1 Spatial Variability of PM Deposition

PM deposition exhibits strong spatial heterogeneity, controlled by emission intensity, proximity to source, and wind dynamics. Fluxes range from 33.7 to 9,336.0 µg/cm²/day (mean ≈ 2,187 µg/cm²/day; CV ≈ 170%), indicating a highly uneven, point-source dominated distribution.

Table 1: Spatial and Seasonal Variation of PM Deposition

Station	Direction	Dry (µg/cm²·day)	Wet (µg/cm²·day)	Mean (µg/cm²·day)
PMS1	Downwind	70.0	46.6	58.3
PMS2	Downwind	1,148.4	765.6	957.0
PMS3	Upwind	40.4	27.0	33.7
PMS4	Upwind	228.4	152.2	190.3
PMS5	Downwind	161.4	107.6	134.5
PMS6	Upwind	936.6	624.4	780.5
PMS7	Downwind	11,203.2	7,468.8	9,336.0
PMS8	Downwind	1,207.0	804.6	1,005.8
PMS9	Upwind	8,621.4	5,747.6	7,184.5

Peak deposition occurs at PMS7 (9,336.0 µg cm^{-2} day^{-1}) and PMS9 (7,184.5 µg cm^{-2} day^{-1}) within the near-field zone (<1 km) (Table 1), reflecting intense localized fallout from operational hotspots. Deposition declines with distance, consistent with gravitational settling and atmospheric dilution, while low values at PMS1 and PMS3 (<100 µg cm^{-2} day^{-1}) indicate minimal distal influence.

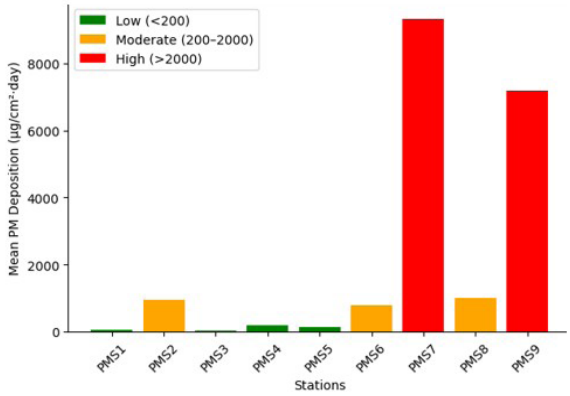

Figure 2: Spatial variability of PM deposition (low–moderate–high zones)

Categorization identifies three zones (Figure 2): low (<200), moderate (200–2000), and high (>2000 µg/cm²/day). High deposition is concentrated at PMS7 and PMS9, whereas low deposition occurs at distal stations, confirming a distance-decay, anisotropic, and source-driven pattern.

Directional analysis shows slightly higher deposition in downwind locations (2,298.3 µg/cm²/day) relative to upwind areas (2,047.3 µg/cm²/day), confirming wind-driven transport. However, similarly high variability (CV > 160%) in both zones indicates additional dispersion processes, including turbulence and dust re-suspension. Peak deposition in the downwind zone (9,336.0µg/cm²/day) highlights localized emission dominance.

PM deposition is higher in the dry season (2,624.1µg/cm²/day) than in the wet season (1,749.6µg/cm²/day), reflecting enhanced atmospheric stability and reduced wet scavenging. Persistently high variability (CV ≈ 175%) indicates that spatial controls outweigh seasonal influences.

3.2. Heavy Metal Distribution across Soil, Surface Water, and Groundwater

Heavy metal distribution across environmental media indicates a clear pattern of cross-media contamination, driven by atmospheric deposition, runoff, and subsurface transport. Mean concentrations (Figure 3) show that surface water is the most impacted medium, followed by soil and then groundwater, reflecting decreasing mobility and increasing attenuation with depth.

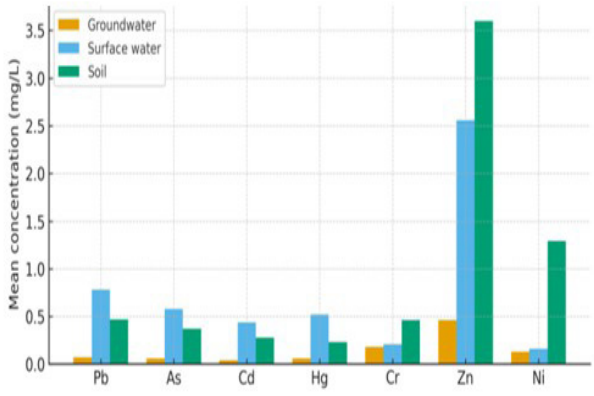

Figure 3: Mean Heavy Metal Concentrations across Sample Types.

Surface water exhibits the highest metal concentrations, with Pb (0.78 mg L^{-1}), Cd (0.44 mg L^{-1}), As (0.58 mg L^{-1}), Hg (0.52 mg L^{-1}), and Zn (2.56 mg L^{-1}) far exceeding WHO/NIS limits. This reflects rapid mobilization via dust wash-off, runoff, and possible wastewater inputs, supported by elevated TSS (9.00 mg L^{-1}) and TDS (609.67 mg L^{-1}), which enhance metal transport and solubility.

Soils show substantial enrichment of Pb (0.47 mg L^{-1}), Cd (0.28 mg L^{-1}), As (0.37 mg L^{-1}), Cr (0.46 mg L^{-1}), Ni (1.29 mg L^{-1}), and Zn (3.60 mg L^{-1}), indicating long-term accumulation from particulate deposition. Near-neutral pH and carbonate-rich conditions favor metal retention, while also enabling gradual release under changing hydrochemical conditions, making soils a secondary contamination source.

Groundwater contains lower but still elevated concentrations of Pb (0.07 mg L^{-1}), Cd (0.04 mg L^{-1}), As (0.06 mg L^{-1}), Cr (0.18 mg L^{-1}), and Zn (0.46 mg L^{-1}), confirming vertical migration through infiltration and leaching. Although attenuation processes reduce concentrations, the presence of these metals indicates vulnerability of the aquifer system.

Generally, the observed enrichment follows the trend: Surface water > Soil > Groundwater. This reflects dominant surface transport processes and progressive subsurface attenuation. Element-specific patterns suggest Pb and Cd are primarily linked to cement dust and industrial activities, As and Hg to combustion-related inputs, and Zn and Ni to particulate accumulation in soils. These results demonstrate a connected contamination system, where particulate deposition and hydrochemical processes jointly control metal distribution across media, posing significant risks to water quality and agricultural systems.

3.3 Physicochemical and Hydrochemical Characteristics

The physicochemical and hydrochemical profiles (Table 2) indicate clear ionic enrichment and alkalinization across environmental media, with the strongest impact observed in surface water. Elevated EC (872.33 µS cm^{-1}) and TDS (609.67 mg L^{-1}) in surface water reflect enhanced solute loading from particulate dissolution and runoff, while comparatively lower values in groundwater (EC = 280.20 µS cm^{-1}; TDS = 127.92 mg L^{-1}) indicate attenuation through subsurface processes.

Table 2: Mean Physicochemical Parameters and Trace Metals across Sample Types

Parameter	Mean		
	Ground-water	Surface Water	Soil
EC (µS/cm)	280.20	872.33	242.21
pH	6.92	7.24	7.04
TSS (mg/L)	0.16	9.00	9.10
SO_4^{2-} (mg/L)	13.04	16.33	12.37
Ca^{2+} (mg/L)	9.03	9.12	17.99
Mg^{2+} (mg/L)	4.84	5.10	3.86
Na^{+} (mg/L)	1.19	0.51	0.92

Cl^- (mg/L)	22.00	22.00	30.64
Cu (mg/L)	0.29	1.46	1.28
TDS (mg/L)	127.92	609.67	105.75
Free Chlorine (mg/L)	0.81	13.66	1.57
Pb (mg/L)	0.07	0.78	0.47
Zn (mg/L)	0.46	2.56	3.60
As (mg/L)	0.06	0.58	0.37
Cd (mg/L)	0.04	0.44	0.28
Cr (mg/L)	0.18	0.21	0.46
Hg (mg/L)	0.06	0.52	0.23
Mn (mg/L)	0.06	0.43	0.06
PO_4^{3-} (mg/L)	0.15	0.33	0.85
Ni (mg/L)	0.13	0.16	1.29
Turbidity (NTU)	1.77	31.33	34.45
Total Hardness (mg/L)	39.86	27.67	43.04
Carbonate (mg/L)	22.00	161.67	256.79
Bicarbonate (mg/L)	53.48	303.33	159.64
Total Alkalinity (mg/L)	110.57	97.24	116.96
Total Solids (mg/L)	130.36	134.55	128.98

pH values across all media (6.92–7.24) are near-neutral to mildly alkaline, consistent with inputs of Ca–Mg–SO_4^{2-}-rich cement dust. This is further supported by elevated carbonate (up to 256.79 mg L^{-1}), bicarbonate (303.33 mg L^{-1}), and total alkalinity, particularly in soils and surface water, indicating progressive alkalinization and buffering capacity enhancement.

Major ions exhibit distinct distribution patterns: Ca^{2+} and Mg^{2+} are enriched in soils (17.99 and 3.86 mg L^{-1}), reflecting mineral accumulation and adsorption, while Cl^- and Na^+ show relatively stable concentrations across media, suggesting limited anthropogenic perturbation. Elevated turbidity (31.33–34.45 NTU) and TSS (~9 mg L^{-1}) in surface water and soils indicate high particulate loading, facilitating metal transport.

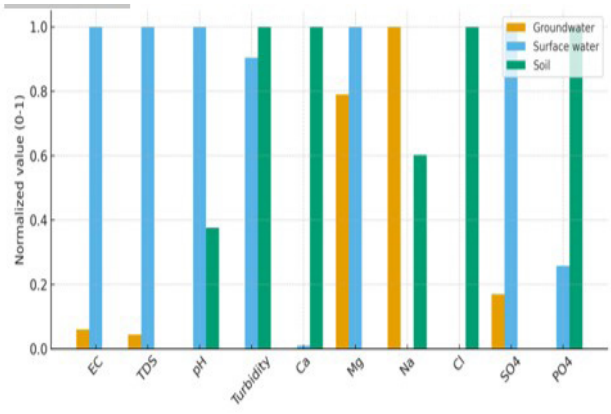

Figure 4: Normalized Physicochemical Parameters across Sample Types.

Normalized comparisons (Figure 4) reinforce these trends, showing that EC, TDS, and pH peak near emission zones and decline with distance, confirming a spatial gradient controlled by PM deposition intensity. This pattern demonstrates that particulate fallout drives localized ionic enrichment and hydrochemical modification, particularly through increased Ca^{2+}, Mg^{2+}, and SO_4^{2-} inputs. The hydrochemical system reflects a coupled particulate–aqueous interaction, where cement dust deposition alters water chemistry, enhances alkalinity, and promotes metal mobility and retention. These relationships highlight the role of physicochemical conditions in governing contaminant transport and distribution across impacted soils and water systems.

3.4 Relationships between PM Deposition, Ionic Enrichment, and Metal Mobility.

Correlation analysis reveals a strong coupling between particulate deposition, ionic enrichment, and metal mobility within the study area. Elevated EC (872.33 µS cm^{-1}) and TDS (609.67 mg L^{-1}) in surface water indicate significant solute enrichment from cement dust dissolution and runoff, further supported by high turbidity (31.33 NTU), which reflects active particulate transport.

A strong positive correlation between EC and TDS ($r = 0.85$, $p < 0.01$) confirms that both parameters are governed by the same dust-derived ionic inputs, primarily Ca^{2+} and SO_4^{2-}. The significant relationship between PM deposition and Pb ($r = 0.62$) demonstrates the direct role of atmospheric fallout in metal loading across environmental media, linking emission sources to observed contamination.

Additionally, the moderate correlation between EC and Cd ($r = 0.52$) indicates that increasing ionic strength enhances metal solubility and mobility, particularly under mildly alkaline conditions. This suggests that cement-derived ions not only accumulate in solution but also facilitate desorption of metals from soil and particulate surfaces, increasing their bioavailability.

Collectively, these relationships demonstrate a coupled hydrogeochemical system, where PM deposition drives ionic enrichment, which in turn modifies geochemical conditions to enhance metal mobilization and cross-media transfer. This interaction provides quantitative evidence of dust-induced hydrochemical alteration and contaminant transport in the study area.

3.5 Discussion

The results substantiate the study hypothesis that cement-derived PM deposition is a primary driver of

cross-media contamination, exerting coupled control on heavy metal enrichment, hydrochemical alteration, and contaminant mobility. The observed spatial gradients, characterized by near-field deposition maxima and strong heterogeneity, confirm that emission intensity and wind-driven dispersion govern particulate distribution and subsequent environmental loading.

Consistent with the hypothesis, elevated concentrations of Pb, Cd, As, and related trace metals across soil, surface water, and groundwater demonstrate that PM deposition significantly enhances heavy metal accumulation across environmental media. The distribution pattern further indicates that deposited particulates act both as immediate contamination inputs and as secondary reservoirs, sustaining progressive leaching and subsurface transfer.

Hydrochemical responses provide direct evidence of dust-induced alteration. Increased EC, TDS, and alkalinity reflect dissolution of cement-derived Ca^{2+}, Mg^{2+}, and SO_4^{2-}, confirming that PM deposition induces measurable ionic enrichment. The resulting near-neutral to mildly alkaline conditions favor cation exchange and destabilization of metal-binding phases, thereby enhancing metal solubility-precisely as hypothesized

The statistical relationships reinforce this coupled mechanism. The strong EC–TDS correlation ($r = 0.85$, $p < 0.01$) verifies a common ionic source linked to particulate inputs, while the PM–Pb relationship ($r = 0.62$) confirms atmospheric control of metal loading. The positive EC–Cd association ($r = 0.52$) further demonstrates that increased ionic strength promotes metal desorption and mobility. These interactions validate the hypothesis that PM deposition exhibits significant positive relationships with trace metal enrichment and governs contaminant transport through hydrochemical modification.

Collectively, the findings define a coherent process pathway: particulate deposition elevates ionic strength and alkalinity, which in turn enhances metal mobilization and facilitates cross-media transfer (PM deposition → ionic enrichment (EC/TDS increase) → soil alkalinization → metal mobilization → cross-media transfer → hydrochemical degradation). This dust-mediated hydrochemical coupling explains the observed exceedances and aligns with established behavior in cement-impacted systems.

Cement production therefore emerges as the dominant forcing factor controlling environmental degradation in the study area. The quantified linkages between PM deposition, ionic enrichment, and metal mobility provide a robust mechanistic basis for predictive modelling and targeted mitigation, emphasizing the need for integrated emission control and hydrochemical management to reduce long-term ecological and public health risks.

4. CONCLUSION

The following conclusions were drawn from the study:

Hydrochemical degradation in the studied industrial corridor is driven by cement-derived particulate deposition and ionic enrichment, with elevated PM fluxes and exceedance of Pb, Cd, As, and Hg confirming cement dust as the dominant contamination pathway, spatially controlled by source proximity and atmospheric dispersion.

Increased EC and TDS from Ca^{2+}–Mg^{2+}–SO_4^{2-} inputs modify geochemical equilibria and enhance metal solubility, desorption, and leaching, with strong EC–TDS and PM–metal correlations demonstrating a coupled particulate–ionic mechanism governing contaminant transport.

A process linkage between deposition, alkalinization, and metal mobilization drives cross-media contamination of soil and water resources.

The findings provide a quantitative basis for integrated emission control, hydrochemical monitoring, and predictive risk modelling, essential for mitigating long-term environmental and public health risks in cement-producing regions.

REFERENCES

Adagba, T., Oguche, P., & Usman, A. (2022). Assessment of irrigation water quality and hydrochemical characterization of groundwater in North-Central Nigeria. Environmental Monitoring and Assessment, 194, 812.

Adebayo, O. A., Eze, C., & Musa, Y. (2023). Hydrogeochemical characterization and heavy metal pollution indices of groundwater around cement industries in Nigeria. Journal of Environmental Management, 332, 117433.

Adeniyi, A. H., Haliru, A. K., Zango, Z. U., Akpambang, V. O. E., & Nura, A. Y. (2022). Assessment of ambient air quality in Obajana cement industry, Kogi State, Nigeria. Ethiopian Journal of Environmental Studies and Management, 15(5), 630–641.

APHA. (2017). Standard methods for the examination of water and wastewater (23rd ed.). American Public Health Association.

ASTM. (2001). ASTM D4448-01: Standard guide for sampling ground-water monitoring wells. ASTM International.

ASTM. (2002). ASTM D6044: Standard guide for representative sampling for hazardous waste and contaminated media investigation. ASTM International.

Etim, E. U., Akpan, E., & Umoh, I. (2021). Airborne particulate matter and its environmental implications around cement industries in Nigeria. Environmental Monitoring and Assessment, 193(4), 259. https://doi.org/10.1007/s10661-021-08971-0

Ibrahim, M. A., Lawal, R., & Ojo, J. (2021). Environmental assessment of cement dust pollution and its effect on soil fertility in Kogi State, Nigeria. Scientific African, 13, e00891. https://doi.org/10.1016/j.sciaf.2021.e00891

Ismail, A. (2023). Cement dust pollution and its environmental impacts: A review. Environmental Science and Pollution Research.

Minkina, T. M., Mandzhieva, S. S., & Bauer, T. V. (2018). Soil contamination and remediation: Heavy metals, organic pollutants, and radionuclides. CRC Press.

NiMet (Nigerian Meteorological Agency). (2023). 2023 seasonal climate prediction for Nigeria. Federal Ministry of Aviation, Abuja.

Obaje, N. G. (2009). Geology and mineral resources of Nigeria. Springer.

Ogunbiyi, A. O., Olatunbosun, O. A., & Adeyemi, A. A. (2022). Evaluation of cement dust impact on soil and water quality in industrial zones of North-Central Nigeria. Environmental Monitoring and Assessment, 194(8), 634. https://doi.org/10.1007/s10661-022-10227-0

Ogundele, L. T., Adejumo, I. A., & Awomeso, J. A. (2020). Air quality indices and human health risk assessment around Nigerian cement plants. Environmental Science and Pollution Research, 27(6), 6724–6737.

Ogunkunle, C. O., Fatoba, P. O., & Oyedele, D. (2021). Soil and plant contamination from cement dust: Health risk implications in Nigeria. Environmental Geochemistry and Health, 43, 2769–2785. https://doi.org/10.1007/s10653-020-00688-2

Okoro, C. C., Anake, W. U., & Adebayo, A. O. (2022). Heavy metal accumulation in soils and crops around cement industries in Nigeria. Environmental Challenges, 7, 100528. https://doi.org/10.1016/j.envc.2022.100528

Olatunbosun, O. A., Adebayo, A. O., & Olayinka, K. O. (2020). Assessment of heavy metal pollution indices in soils around industrial zones in southwestern Nigeria. Environmental Earth Sciences, 79(5), 153.

USEPA. (2016). Air quality criteria for particulate matter (EPA/600/R-15/072). U.S. Environmental Protection Agency.

WHO. (2013). Health effects of particulate matter: Policy implications for countries in Eastern Europe, Caucasus and Central Asia. World Health Organization.

Yang, X., Li, Z., Wang, Y., & Chen, J. (2024). Atmospheric particulate matter deposition and associated heavy metal contamination in industrial regions. Science of the Total Environment.